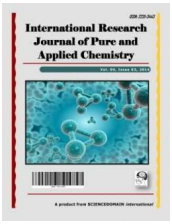

International Research Journal of Pure & Applied Chemistry
14(1): 1-15, 2017; Article no.IRJPAC.33073
ISSN: 2231-3443, NLM ID: 101647669

SCIENCEDOMAIN *international*
www.sciencedomain.org

Adsorption of 2, 4 Dichlorophenoxyacetic Acid on Different Types of Activated Carbons Based Date Palm Pits: Kinetic and Thermodynamic Studies

A. M. Youssef [1], H. EL-Didamony[2], S. F. EL- Sharabasy[3], M. Sobhy[1,3*], Asaad F. Hassan[4], Roman Buláneke[5]

[1]Department of Chemistry, Faculty of Science, Mansoura University, Mansoura, Egypt.
[2]Department of Chemistry, Faculty of Science, Zagazig University, Zagazig, Egypt.
[3]Central Laboratory of Date Palm Research and Development, Agricultural Research Center, Egypt.
[4]Department of Chemistry, Faculty of Science, Damanhour University, Damanhour, Egypt.
[5]Department of Physical Chemistry, Faculty of Chemical Technology, University of Pardubice, Czech Republic.

Authors' contributions

This work was carried out in collaboration between all authors. Authors AMY, HED and SFES wrote the protocol for research paper. Authors MS and AFH were responsible for experimental work, managed the literature search and the preparation of manuscript. Author RB was responsible for the analysis of nitrogen adsorption and texture characterization part. All authors read and approved the final manuscript.

Article Information

DOI: 10.9734/IRJPAC/2017/33073
Editor(s):
(1) Surendra Reddy Punganuru, Department of Biomedical Sciences, School of Pharmacy, Texas Tech University Health Sciences Center, Amarillo, USA.
Reviewers:
(1) Vito Rizzi, University of Bari, Italy.
(2) O. D. Adeniyi, Federal University of Technology, Niger State, Nigeria.
Complete Peer review History: http://www.sciencedomain.org/review-history/18810

Original Research Article

Received 29th March 2017
Accepted 19th April 2017
Published 26th April 2017

ABSTRACT

The removal of 2,4-dichlorophenoxyacetic acid (2,4-D) from waste water was studied by three activated carbon samples (AP21, AZ21 and AN13) prepared from date palm pits (DP) as a precursor and phosphoric acid, zinc chloride and sodium hydroxide as activating agents. Different techniques were used to characterize the solid adsorbents as N_2-adsorption at −196℃, scanning electron microscopy (SEM), thermo gravimetric analysis (TGA) and FT-IR. The effect of various operating parameters such as initial concentration of 2, 4-D, contact time, temperature, adsorbent

**Corresponding author: E-mail: mahasobhy1000@yahoo.com;*

dosage, and pH were investigated. Equilibrium isotherms were used to identify the possible mechanism of the adsorption process. Characterization results showed that AN13 sample gave the heights surface area 498.9 m^2/g and micropores volume 0.239 cm^3/g. pH_{pzc}, pH of the supernatant and FT-IR indicated the presence of different C-O function groups. It was shown that the adsorption of 2, 4-D on activated carbon samples could be best fitted to Langmuir equation with q_m 80 mg/g in case of AN13. The kinetic data were also examined with applying pseudo-first-order and pseudo-second-order kinetics models and was found to follow closely the pseudo-second-order kinetic model. Thermodynamic parameters such as enthalpy changes (Δ H°), entropy changes Δ S° and free energy changes (Δ G°) were evaluated indicating that the nature of adsorption was found to be endothermic and spontaneous.

Keywords: Activated carbon; date palm pits; 2,4-D; kinetics; thermodynamics.

1. INTRODUCTION

Pollution of surface and ground water with pesticides cause risks to environment and human health. Pesticides is defined as any substance that is used for destruction or control of pests, it includes insecticides, herbicides and fungicides. 2,4-Dichlorophenoxyacetic acid (2,4-D) is a white to yellow crystalline powder and usually present in mixtures of agricultural commercial herbicides and pesticides that are applied to broadleaf weeds, wheat, corn, lawn, and roadsides [1,2]. 2,4-D is one of 188 compounds listed as a Hazardous Air Pollutant (HAP) under section 112(b) [3]. There are over 1,500 pesticide and herbicide products that contain 2, 4-D as the main ingredient. The U.S. EPA Office of Pesticide Programs estimated that total domestic U.S. annual usage of 2,4-D is approximately 46 million pounds with 66% of use in agricultural applications. 2,4-D is also used in Minnesota, Washington, and the New England region to control weed growth in lakes [4], the highest concentrations are found in the water in the first 24 hours after application. Exposure to 2, 4-D can cause blood, liver, and kidney toxicity [4,5]. There are several methods that have been used for the removal of pesticides from aqueous solutions such as photocatalytic degradation [6], ultrasound technology [7,8], electrocoagulation process [9], combined photo-Fenton, biological oxidation [10-13] and nano filtration [14]. Nowadays, adsorption process is widely used for the treatment of the waters contaminated by insecticides [15], it is considered as the most frequently applied methods because of its efficiency, capacity and applicability on a large scale. The most commonly used adsorbent in adsorption process is activated carbon; it is widely used due to its good mechanical strength, chemical stability in diverse media and large pore size distribution in addition to its extensive specific surface area [16]. Activated carbon can be manufactured using different agricultural wastes as it is low-cost sorbents, available and renewable. DP is also used as precursor for production of activated carbon. The world production of dates is about 16,696.56 million tons yearly [17]. Various studies have been reported about the adsorption of 2,4-D from aqueous solution using granular activated carbon prepared from agricultural by products [18,19].

The focus of this research is to compare between three different activated carbons namely: zinc chloride, phosphoric acid, and sodium hydroxide activated carbon based on date palm pits to remove 2,4 D from waste water, the effect of initial concentration, contact time, temperature, and initial pH will be investigated. Furthermore, equilibrium isotherms, kinetic models and thermodynamic parameters will be used to identify the possible mechanism of the adsorption process.

2. MATERIALS AND METHODS

2.1 Materials

A Sawi date palm pits (DP) were collected from pastry factory in Shubra Al Khaimah Cairo, Egypt. The date palm pits were washed with hot deionized water to remove any impurities, dried at 105℃. Raw materials were ground into fine particles and sieved to a particle size of 2 mm. Phosphoric acid, zinc chloride, sodium hydroxide and 2,4 dichlorophenoxy acetic acid were of analytical grade and were obtained from Sigma-Aldrich Company (China). All chemicals were used without further purifications. Deionized distilled water was used for all experiments.

2.2 Preparation of Activated Carbons

Phosphoric acid and zinc chloride activated carbon were prepared by soaking the particle of

dried date palm pits in H_3PO_4 or $ZnCl_2$ by ratio 2:1 (precursor : activating agent) using suitable amount of water for 48 h. Then the mixture was dried at 110℃ for 24 h. The dried solid was pyrolysis in absence of air in stainless steel reactor (60× 4 cm) at rate of heating 10℃/min up to 550℃ and maintained at that temperature for 4 h, cooling to room temperature and the produced activated carbon mass washed with deionized water till pH of washing solution attained ~6.0. The washed activated carbons were dried at 110℃ for 24 h [20], stored in clean dry bottles and named AP21 and AZ21. Carbonized sample (C) was prepared by calcination of DP in absence of air at constant temperature (600℃) for 4 h using stainless steel reactor tube (60× 4 cm), the carbonized sample maintain at these temperature for 4 h. Sodium hydroxide activated carbon (AN13) was prepared by soaking the carbonized product (C) in NaOH solution with ratio 1:3 (carbonized sample: NaOH) for 48 h using the least amount of distilled water to dissolve the required quantity of solid NaOH. Then the mixture dried at 110℃ for 24 h. The dried product was heated in the previously stainless steel tube at 750℃ for 4 h, cooling and washing as discussed.

2.3 Characterization of Activated Carbon Samples

2.3.1 Thermal characterization

A thermo gravimetric analysis (TGA) of DP and AN13 activated carbon samples was performed in a thermo-analyzer (NETZCH STA 409-Germany) apparatus at a Helium flow rate of 50 mL/min and a heating rate 15℃/min up to 900℃.

The percentage of ash contents were carried out on DP, AP21, AZ21 and AN13. For each sample a crucible was placed in furnace at 650 ^{o}C for 1 h, cooled down in a desiccator and the weight of ignited crucible was recorded, 2.0 g of activated carbon sample was placed in a crucible and transferred into a muffle furnace at 650℃ for 6 h. After heating, the crucible was allowed to cool to room temperature in desiccator. The percentage ash content was determined using Eq (1) [21].

$$\% \text{ Ash content} = \frac{\text{Weight of ash (g)}}{2.0} \times 100 \qquad (1)$$

2.3.2 Chemical characterization

pH of supernatant was determined by adding 0.5 gm of adsorbent to 25 mL of deionized water and the mixture was shaking for 48 h, the supernatant was then filtered to remove solid adsorbent and the pH of the supernatant was measured using (Jenway pH-meter – UK).

pH_{PZC} of activated carbons was also measured as 50 mL of 0.01 M NaCl solutions was put into several closed Erlenmeyer flasks. The pH in each flask was adjusted to a value between 2 and 12 by adding HCl (0.01 M) or NaOH (0.01 M) solutions. 0.15 g from the sample was added to each flask, the flasks were agitated for 48 h, and the final pH was then measured. The pH_{pzc} is the point where $pH_{final} - pH_{initial}$ = zero [22].

The surface functional groups of the activated carbon samples were identified by Fourier Transform Infrared (FT-IR) spectroscopy analysis using Mattson 5000 FT-IR spectrometer. The pellet for infrared studies was prepared by mixing a given sample with KBr crystals and pressed into a pellet. The pellet which is homogeneous in appearance was inserted into the IR sample holder for the analysis. FT-IR spectra of different samples were recorded within 400 - 4000 cm^{-1}.

2.3.3 Texture characterization

The surface area (S_{BET}, m^2/g) and average pore size of samples were determined using a gas sorption analyzer. The adsorption-desorption isotherm of nitrogen was determined at its boiling point -196℃ by (ASAP 2020 instrument – USA). The samples were degassed under vacuum at 350℃ for 3 h prior to measurement. The adsorption equilibrium time was set at 60 S. Average pore radius ($\bar{r}$, nm) was calculated using the following equation:

$$\bar{r}\,(\text{nm}) = \frac{2V_T\,(\text{mL/g})}{S_{BET}\,(\text{m}^2/\text{g})} \times 10^3 \qquad (2)$$

where, V_T is the adsorbed volume near saturation, i.e. at p/p° ~ 0.95 multiplied by the factor 15.5 ×10^{-4}. The surface morphology of the of the activated carbon samples was examined using Scanning Electron Microscope (SEM) model (Quanta 250 FEG) working at a high voltage of 15 kV to generate a variety of signals at the surface of solid sample. Before the measurements, the sample was dried at 110℃ for 4 h. The sample was coated with a thin layer of gold for charge dissipation.

2.4 Adsorption Studies of 2,4 D

Batch adsorption equilibrium experiments were conducted for the adsorption of 2,4 D on

activated carbons by adding 0.25 g of dried activated carbon to 50 mL of 2,4 D solution with different concentrations (50-400 mg/L) at constant shaking speed (175 rpm). Then the mixture was filtered and the residual 2,4 D concentrations were measured at a wavelength of 283 nm using a double beam UV–visible spectrophotometer (UV-1700 Shimadzu, Japan). Adsorbed amount q_e (mg/g) was calculated as follows:

$$q_e = \frac{(C_o - Ce)V}{M} \quad (3)$$

Where C_o and C_e are the initial and equilibrium liquid phase concentration of 2, 4-D (mg/L), respectively. V is the volume of solution (L), and M is the amount of adsorbent used (g). To study the influence of pH on the adsorption of 2,4 D; the experiments were conducted at different pH ranged from 2 to 10 at constant initial 2,4 D concentration of 200 mg/L. The pH of each solution was adjusted using 0.1 M NaOH or 0.1 M HCl. The concentrations of 2,4 D was determined using a double beam UV–visible spectrophotometer (UV-1700 Shimadzu, Japan).

Effect of time was carried out by contacting 0.25 g of adsorbent with 50 mL of 2,4 D solution of definite concentration of adsorbate 200 mg/L. The concentration of adsorbate after recorded time intervals (C_t) is determined; the adsorption capacity at time t, q_t (mg/g) was calculated using Eq (4)

$$q_t = \frac{(C_o - C_t)V}{M} \quad (4)$$

The similar procedures were followed for another three sets of Erlenmeyer flask containing the same initial concentration of 2,4-D and the same activated carbons dosage, but were kept under 25, 35 and 45℃ for studying the effect of adsorption temperature and calculating the thermodynamic parameters.

3. RESULTS AND DISCUSSION

3.1 Thermal Characterization

Thermogravimetric analysis is important technique used to study thermal stability and inorganic contents of precursor before preparation of activated carbons. Fig. 1 shows TGA curves for DP and AN13. For DP sample at temperature below 150℃, there is no observable mass loss, while in case of AN13 sample the weight loss was observed to be 6% and that is due to the loss of adsorbed moisture by C-O function groups created on activated carbon sample and higher surface area. The significant weight loss for DP was observed between 250-400℃ and this represent about 55%, this is due to cellulose and hemicellulose decomposition. The weight loss in range 415-750℃ represents about 59% due to the decomposition of lignin component that degrades slowly and cover wide range of temperature [23]. AN13 sample shows high thermal stability compared with DP due to preactivation at high temperature. At 800- 900℃, the mass loss was 24%; these values represent the largest mass loss which is due to loss of residual lignin in activated carbon sample.

The ash content for DP was found to be 0.77% (Table 1) which is very low due to the higher amount of cellulose and lignin [24]. While for activated carbon samples it is in the range of 2.39-5.17 due to the presences of different activating agent which has the ability to dissolve part of carbon content in samples followed by an increase in ash content.

3.2 Chemical Characterization

Surface chemistry of a solid adsorbent is a very important factor in the determination of the adsorption capacity and in identifying the chemical nature of the activated carbon surface. The values of pH_{pzc} and pH of supernatant are listed in Table 1 for all samples. These give information about C─O surface groups created on the surface during activation [25]. Activation with $ZnCl_2$ or H_3PO_4 creates acid function groups as reported by the lower pH_{pzc} values; while pH_{pzc} for AN13 was found to be 8.65 and this means base functional group predominate on the surface of the sample.

FT-IR is mainly used as a qualitative technique for the study of surface chemical functional groups on activated carbons. Fig. 2 shows the FT-IR spectra of DP, AP21, AZ21 and AN13. The observation of absorption bands shows that the difference between DP and activated carbons is mainly due to the formation of oxygen function group for all activated carbon samples. The band around 3500-3400 cm^{-1} is due to the –OH stretching vibration mode of hydroxyl functional groups and adsorbed water [26]. Acidic treatment reduces the hydroxide groups and produces acidic functional groups on the surface of chemically activated carbon by acid. The peak around 2900─2850 cm^{-1} which is observed in DP

Table 1. Ash content, pH of supernatant and pHpzc for DP, AP21, AZ21 and AN13

Sample	Percentage ash (%)	pH of supernatant	pH_{pzc}
DP	0.770	5.950	6.321
AP21	5.170	2.350	3.202
AZ21	2.520	3.900	5.230
AN13	2.390	8.00	8.650

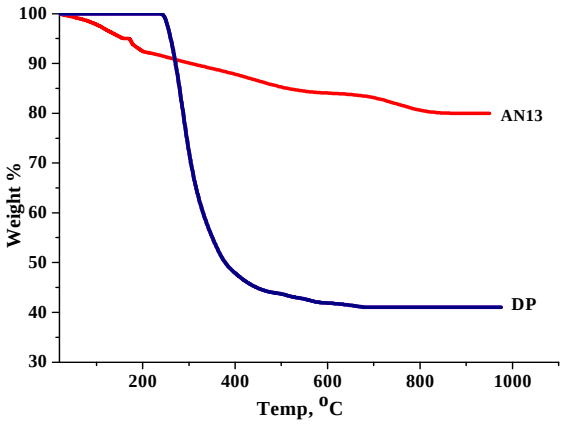

Fig. 1. TGA of date palm pits (DP) and activated carbon sample (AN13)

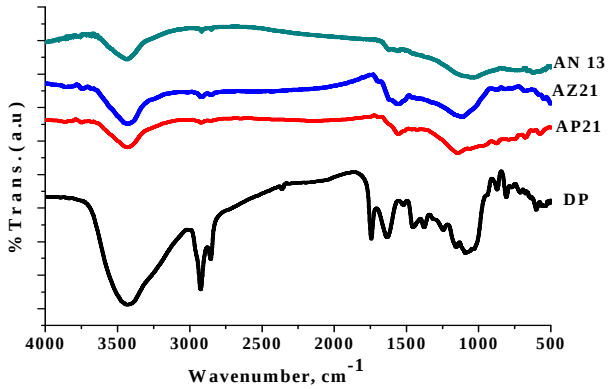

Fig. 2. FT-IR spectra of (DP) and activated carbon samples AP21, AZ21 and AN13

sample indicates the presence of a methylene group (–CH_2–) with –C─H stretching [27]. A small peak at 1772 cm^{-1} in the case of AZ21 and AP21 samples corresponds to the C=O stretching vibration in carbonyls such as ketones, aldehydes, lactones and carboxylic groups [28] and almost absent in the case of AN13 sample. The weak intensity of this peak indicates that the prepared activated carbons contain small amount of carboxyl group. Small peak around 1520 cm^{-1} may refer to the C=C stretching vibration in aromatic rings [29], this is due to the tars produced during depolymerization of cellulose followed by dehydration and condensation contributed to the formation of more aromatic and reactive products with some cross linking [30]. The band in the range of 1000─1300 cm^{-1} is due to vibrations of various C─O bonds such as those in ethers, phenols, and esters [31,32]. Generally, the acidic surface properties are caused by the presence of carboxyl groups, lactones and hydroxyl groups of a phenolic character [33]. Basic groups are corresponding to chromene or pyrone like structures [34].

3.3 Texture Characterization

The adsorption/desorption isotherms at -196℃ for the investigated activated carbon samples was represented in Fig. 3a. It is clear that all activated carbon samples gave hysteresis loop, this hysteresis loop is usually attributed to thermodynamic or network effects or combination of two effects [35]. Also the samples exhibited adsorption isotherm of type I which represent on micro porous solids in that micro pore filling occurs significantly at relatively low pressure < 0.1 (P/P°), the adsorption being completed at 0.5 P/P°. Fig. 3a was used to determine the specific surface area (S_{BET}, m^2/g), total pore volume (V_T, mL/g), and average pore radius ($\bar{r}$, nm). The BET surface area was determined by means of the standard BET equation applied in the relative pressure range from 0.05 to 0.30 [36]. The data are summarized in Table 2 and showed that: (i) Activation with H_3PO_4, $ZnCl_2$ and NaOH raise surface area, total pore volume, micropores volume and pore radius. The last results based on those dehydrating agents penetrate deep into

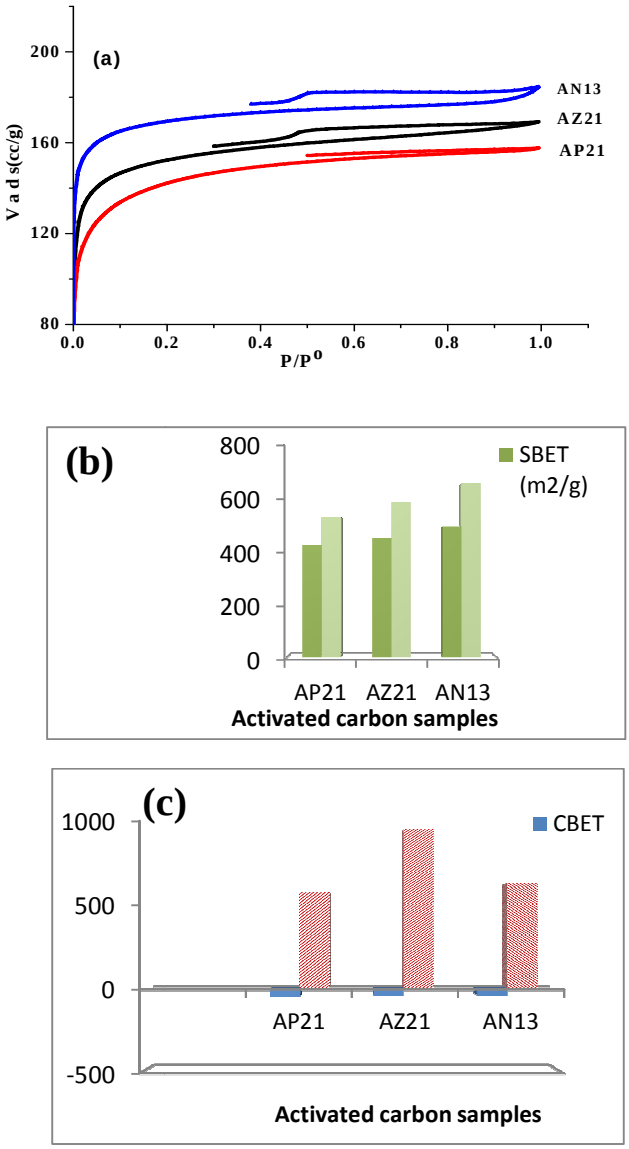

Fig. 3. Nitrogen adsorption isotherms of activated carbon sample at -196℃ (a), Surface area (b) and C constant of sample according to Brunauer-Emmett- Teller equation and Rouquerol (c)

Table 2. Textural properties of the investigated activated carbons as determined from nitrogen adsorption at -196℃

Sample	S_{BET} (m^2/g)	C_{BET}	S_{ROU} (m^2/g)	C_{ROU}	$S_{ext+meso}$ (m^2/g)	C_{MBET}	V_{μ} (cm^3/g)	V_P (cm^3/g)	$\bar{r}$ (nm)
AP21	427.8	-45.05	534.7	586.41	112.3	17.16	0.178	0.243	1.14
AZ21	453.8	-42.9	591.6	969.4	75.1	16.61	0.207	0.260	1.15
AN13	498.9	-39.5	662.7	6398	59.8	17.50	0.239	0.285	1.14

the biomass structure and cause the organic molecules to disintegrate into smaller molecules. After the release of these smaller molecules, tiny pores were created. Besides helping in the development of new pores or expansion of the pore, it also affects in enhancing the surface area. Normally, it was observed that micropores and mesopore formation results into a larger surface area of the activated carbons.(ii) The BET evaluation applied here is only valid in a relative pressure range, in which BET is a linear function with respect to the relative pressure. The typical BET range for numerous mesoporous materials is $0.05 \leq P/P° \leq 0.3$. The BET plot of microporous materials (pore widths below 2 nm) in this classical BET range does not give a straight line and the BET evaluation leads to a negative intercept and a negative CBET value. Therefore, the BET evaluation was not applicable to microporous materials, and " Rouquerol rule" was applied in which the application of the linear plot in relative pressure $0.05 \leq P/P° \leq 0.1$ indicates a positive CROU and higher surface area (SROU) more than SBET as shown in Fig. 3b,c.

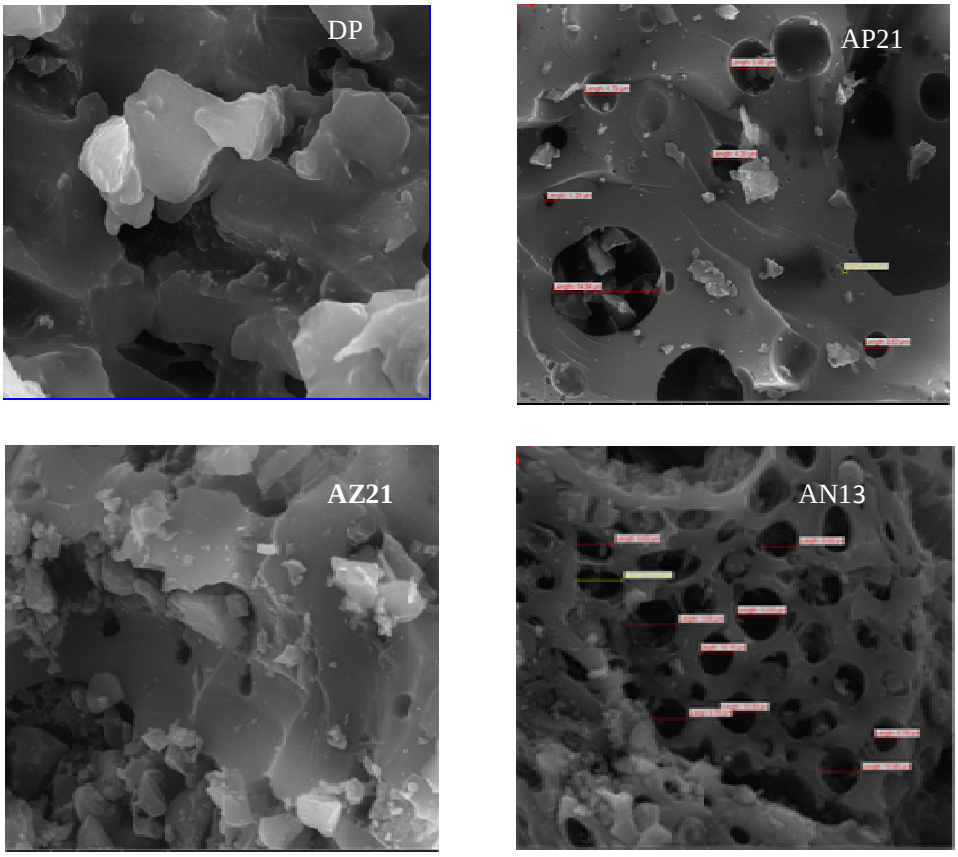

Fig. 4. SEM images of DP, AP21, AZ21 and AN13

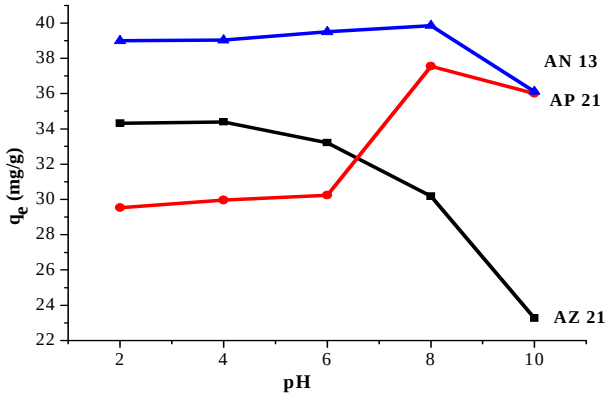

Fig. 5. Effect of pH on adsorption of 2, 4-dichlorophenoxyacetic acid by activated carbon samples. Reaction conditions: temp=25℃, initial 2, 4-D conc=200 mg/L adsorbent dosage=0.25 g, and equilibrium time= 24 h

From the data in Table 2 we can observe that (i) S_{BET} for AN13 is the highest value due to the aggressive effect of NaOH on carbon contents of the carbonized sample creating a new micropores and that is also confirmed by its lower ash content. (ii) Pore radius for all the three samples are in the range of the beginning of mesoporosity range. (iii) Most of the total pore volume is of micropore volume as observed from column 8 and 9 due to the oxidative effect of used activating agents.

Scanning electron microscopy images were taken to observe the surface morphology of the sample. Basically, the pore structure of activated carbon was observed. The micrographs of activated carbon are shown in Fig. 4 showed that chemically activated carbon samples have high porosity compared to DP. This was explained by chemical activation process by phosphoric acid, zinc chloride or sodium hydroxide that responsible for decomposition of organic material to release volatile matter and development of micro porous structure which could increase the adsorption capacity [37].

3.4 Adsorption of 2,4-Dichlorophenoxyacetic Acid

3.4.1 Effect of pH on adsorption of 2, 4-dichlorophenoxy acetic acid

The initial pH of solution is considering one of the most important parameter that affects the properties of adsorbate, adsorbent and the adsorption process. The effect of pH is due to the electrostatic interaction between the surface of activated carbon sample and the deprotonated species of 2,4-D (the anion of the 2,4-D) [38]. The effect of pH on adsorption of 2,4-D by AZ21, AP21 and AN13 samples was studied in the pH range of 2–10 at initial concentration 200 mg/L, and temperature 25℃ (Fig. 5). 2,4- D present as protonated species or deprotonated species (anion) depending on the solution pH. The protonated species is clear when the solution pH is under 2, whereas the deprotonated species is clear when pH is above 4.5. On the other hand, the dissociation constant (pKa) for 2,4-D is 2.64 [39]. Fig. 5 shows that the adsorption capacity of the activated carbon samples to adsorb 2,4-D will be high in acidic media due to electrostatic attraction occurred between the surface and the anion favoring the accumulation of the herbicide anion on the surface of activated carbon samples.

3.4.2 Effect of contact time and kinetic studies

The effect of contact time on 2, 4-D adsorption was investigated at pH 7, initial concentration 200 mg/L and temperature 25℃ for AZ21, AP21 and AN13. Fig. 6a shows that 2, 4-D was absorbed rapidly at early stages. This occurs due to 2, 4-D was rapidly transported into the adsorbent by the unique hexagonal pore structure, and the strong affinity existed between 2, 4-D and the carboxylate groups on the mesoporous carbon. After that, the adsorption rate of 2, 4-D slowdown till reached the equilibrium. This occur due active sites have

been saturated, leading to a decrease in adsorption rate. In order to investigate the adsorption kinetics and mechanism of 2, 4-D adsorption on activated carbon samples. Pseudo-first (Eq. 5) and pseudo-second (Eq. 6) order equations were used to fit the kinetics process.

$$\log(q_e - q_t) = \log q_e - \frac{K_1}{2.303} t \quad (5)$$

$$\frac{t}{q_t} = \frac{1}{K_2 q_e} + \frac{1}{q_e^2} t \quad (6)$$

Where q_e is the equilibrium adsorbed amount (mg/g), q_t is the amount adsorbed at

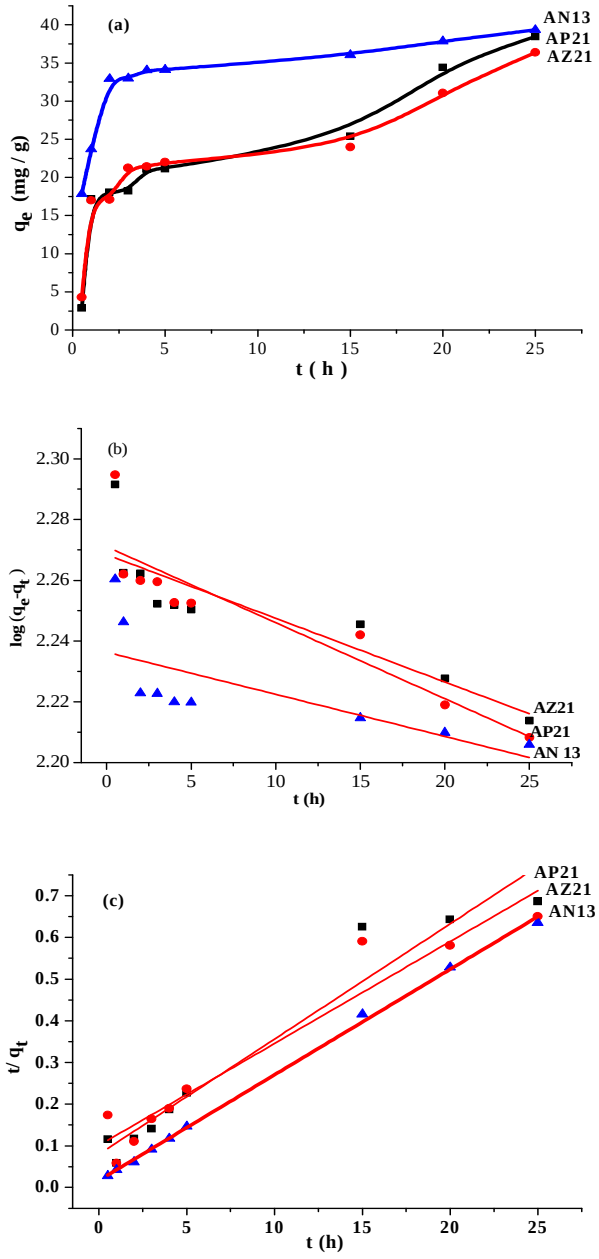

Fig. 6. Kinetic adsorption curves of 2, 4-D by activated carbon samples (a), Pseudo–first (b) and pseudo–second kinetics model(c) for adsorption of 2, 4- D by activated carbon sample at 25℃

Table 3. Kinetic model parameters for adsorption of 2,4-D onto AZ21, AP21 and AN13

Sample	Pseudo–first order kinetic model parameters				Pseudo–second order kinetic model parameters		
	q_m(mg/g)	q_e (mg/g)	K_1 (h^{-1})	R^2	q_e (mg/g)	K_2(g/mgh)	R^2
AZ 21	59.77	185.54	-4.836×10^{-3}	0.7312	36.231	0.00956	0.9405
AP 21	51.02	186.637	-5.7575×10^{-3}	0.7982	40.983	0.00589	0.9227
AN 13	80	172.325	-2.9939×10^{-3}	0.4560	39.478	0.03766	0.9982

time t (mg/g), K1 is the pseudo-first order rate constant (g/mg. min), t is the time in minute and K_2 is the pseudo–second order rate constant (g/mg. min). Fig. 6b and 6c depicts the application of linear pseudo-first-order and pseudo second order kinetics model, respectively and the data was summarized in Table 3. Upon inspection of the data shown in Table 3, we can observe that the adsorption of 2,4 D follow pseudo-second–order kinetics model based on: (i) correlation coefficient R^2 for PSO ranged between 0.9405 and 0.9982 indicating the good applicability of PSO linearized form. On the other hand R^2 for PFO is very low (ranged between 0.4560 and 0.7982) (ii) Calculated q_e (mg/ g) from PSO model are closer to q_m (mg/g) calculated from Langmuir adsorption model while that calculated from PFO is very high.

3.4.3 Adsorption isotherms

The adsorption isotherm indicates how the adsorbed molecules are distributed between the solid surface phase and the liquid phase when the adsorption process reaches an equilibrium state. Several adsorption models have been reported in the literature to describe the adsorption data of isotherms. The amount of 2,4-D adsorbed, q_e (mg/g), is plotted against the equilibrium concentration C_e (mg/L), as shown in Fig. 7a, which indicated that adsorption capacity at equilibrium (q_e) increased for all activated carbon with an increase in the initial pesticide concentrations from 50 to 400 mg/L due to when the initial concentration increased, the mass transfer driving force would become larger, hence resulting in higher adsorption of 2,4-D. The Langmuir and Freundlich are the most frequently used models. In this work the Langmuir model was used to describe the relation between the amounts of 2, 4 -D adsorbed, C_e/q_e, and the equilibrium concentration C_e (mg/L). Langmuir's isotherm model postulates that adsorption occurs on a homogenous surface by monolayer adsorption without interaction between adsorbed molecules, with uniform energies of adsorption on the surface, and no transmigration of adsorbate molecules on the solid surface plane. The linear form of the Langmuir isotherm equation is represented by the following equation [40]:

$$\frac{C_e}{q_e} = \frac{1}{b\, q_m} + \frac{C_e}{q_e} \quad (7)$$

where q_e is the amount adsorbed at equilibrium time (mg/g), C_e is the equilibrium concentration of of 2,4-D (mg/L), q_m is the maximum adsorption capacity (mg/g), and b is known as the Langmuir constant (L/mg) and it is related to the heat of adsorption. The plot of C_e/q_e versus C_e for activated carbon samples (AP21, AZ21 and AN13) will give a straight line with slope = $1/q_m$ and an intercept = $1/bq_m$, as shown in Fig 7b. Freundlich isotherm model is the second most widely used isotherm model and it based on surface heterogeneity. Eq. (8) is the linearized Freundlich form:

$$\ln q_e = \ln K_f + \frac{1}{n} \ln C_e \quad (8)$$

Where K_f and n are Freundlich constants related to adsorption capacity and adsorption intensity, respectively. In general n >1 illustrates that adsorbate is favorable adsorbed on adsorbent whereas n< 1 demonstrates that the adsorption process is chemical in nature, If n lies between 1 and 10, this indicates a favorable sorption process. The plot of ln q_e versus ln C_e gave straight line with slope 1/n and intercept of ln K_f as shown in Fig 7c. The analyzed data will be listed in Table 4 showing that the correlation coefficient, R^2 in case of applying Langmuir model was higher than 0.9695 and dimensionless separation factor(R_L) as represented in Eq. (9) lies between 0-1 so adsorption process will obey Langmuir.

$$R_L = \frac{1}{1 + b\, C_o} \quad (9)$$

while in case of AN13 activated carbon sample showed that both Langmuir and Freundlich are favorable models and this is supported by the

values of R^2 and 1/n of Freundlich which were less than one. The value for 1/n below<1 indicated a Langmuir-type isotherm because it becomes more and more difficult to adsorb additional adsorbate molecules at high concentrations [41], also AN13 sample have high q_m this may be attributed to the acidic nature of 2,4-D and basic nature of AN13 surface.

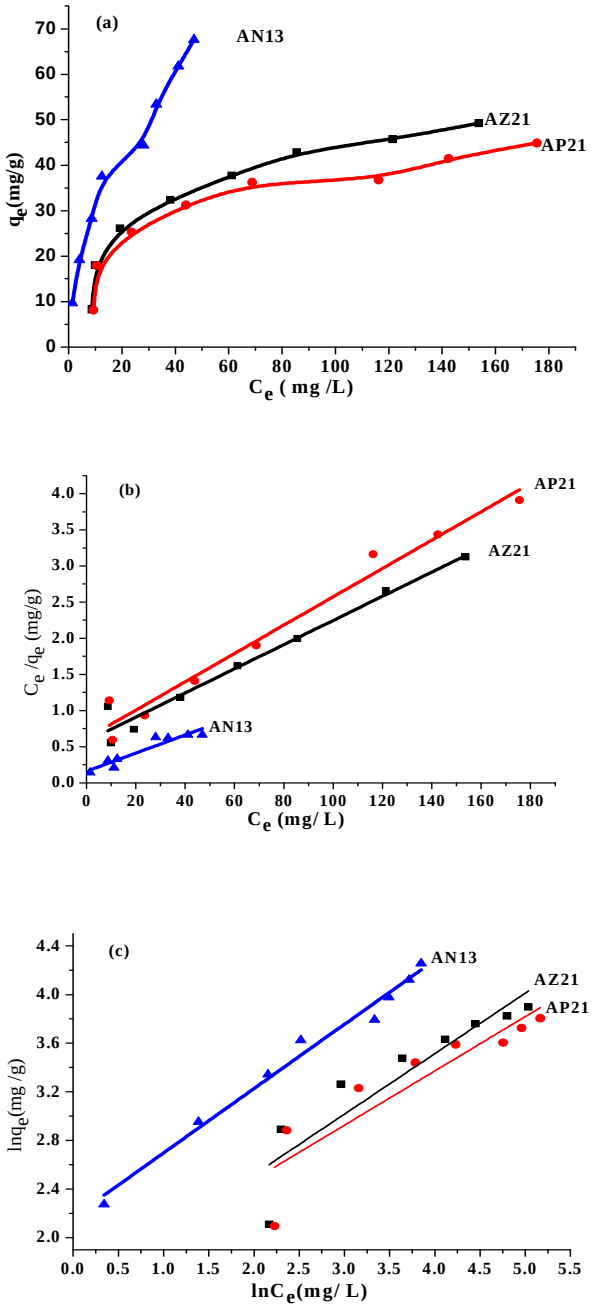

Fig. 7. Adsorption of 2, 4-D onto activated carbon sample (a), Linear Langmuir (b) and Freundlich (c) plot of 2,4 D adsorption on AZ21, AP21 and AN13

Table 4. Langmuir and Freundich constants for 2,4-dichlorophenoxyacetic adsorption at 25℃ by the investigated carbons

Sample	Langmuir parameters				Freundich parameters		
	q_{max}(mg/g)	b(L/mg)	R^2	R_L	K_f(mg/g)	n	R^2
AZ21	59.772	0.0291	0.96471	0.0791	4.5867	2.0092	0.81107
AP21	51.020	0.0755	0.9695	0.0320	4.8792	2.2396	0.78722
CN13	80	0.0788	0.9819	0.0307	8.7523	1.8917	0.9818

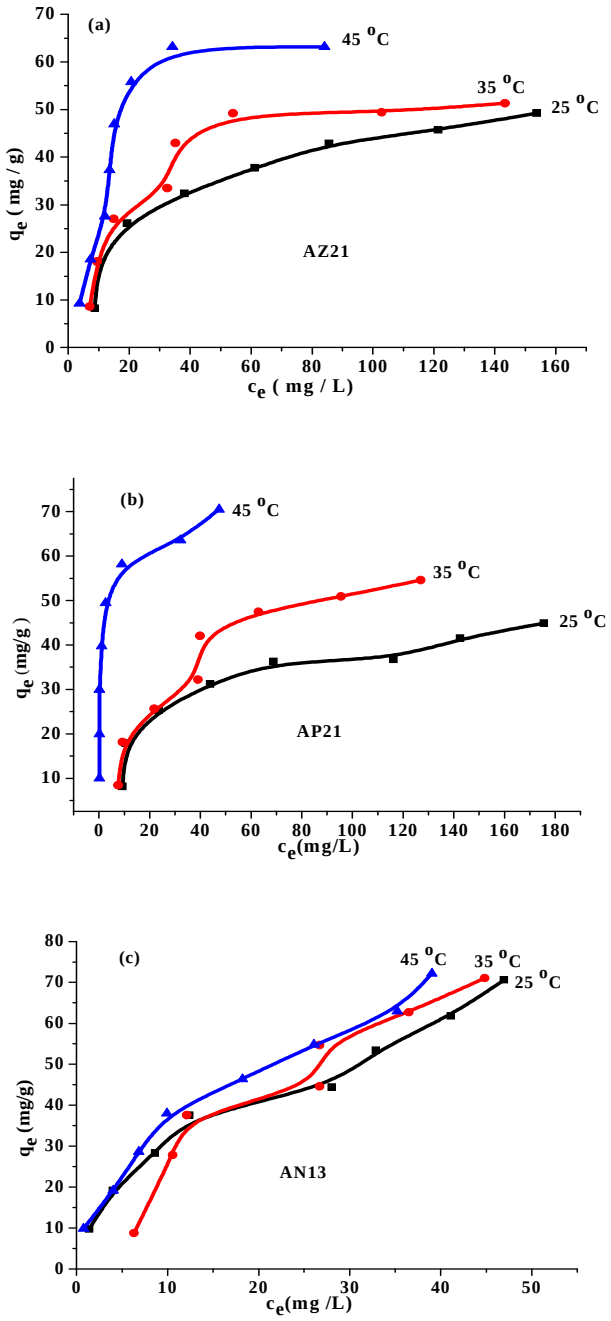

Fig. 8. Adsorption of 2,4-D on AZ21, AP21, and AN13 at 25,35, and 45℃

Table 5. Thermodynamics parameter for adsorption of 2,4-Dichlorophenoxyacetic acid onto AZ21, AP21 and AN13 at 25℃

Sample	ΔS°(kJ mol^{-1} K^{-1})	ΔH°(kJ mol^{-1})	ΔG°(kJ mol $^{-1}$)		
			25°C	35°C	45°C
AZ21	0.1649	45.898	-3.2422	-4.8912	-6.5402
AP21	0.5166	152.32	-1.6268	-6.7928	-11.9588
AN13	0.0535	9.3188	-6.6242	-7.1592	-7.695

3.4.4 Effect of temperature and thermodynamic studies

The effect of temperature on the removal of 2, 4-D was studied at 25, 35 and 45℃. Fig. 8 showed that the ability of activated carbon sample to remove 2, 4-D which increased by raising the temperature from 25 to 45℃ for activated carbon sample and this due to the enlargement of pore size or creation of some new active sites on the surface of adsorbent due to rupture of bond. These also lead to enhancement the transformation of 2, 4-D from the bulk of solution to the surface of adsorbent and penetrate within activated carbon structure overcoming the activation energy barrier and enhancing the rate of intraparticle diffusion [42-44].

Thermodynamic parameters were calculated for AP21, AZ21 and AN13 samples, to explain the nature of adsorption process on the surface and within the pores of activated carbons. The distribution coefficient, Entropy change and Gibbs free energy change of the adsorption process is related to the equilibrium constant by the classic Van't Hoff equation:

$$K_d = \frac{C_s}{C_e} \quad (10)$$

Where K_d is the distribution coefficient for the adsorption, C_s is the surface concentration of 2, 4-D and C_e the equilibrium concentration. According to thermodynamics, the Gibbs free energy change is also related to the entropy change and heat of adsorption at constant temperature by the following equation:

$$\Delta G^\circ = \Delta H^\circ - T\Delta S^\circ \quad (11)$$

$$\Delta G^\circ = - RT \ln K_d \quad (12)$$

Where, R is the universal gas constant (8.314 × 10^{-3} kJ $K^{-1}mol^{-1}$), T is temperature in K. ΔG° is the free energy change (kJ mol^{-1}), ΔH° is the change in enthalpy (kJ mol^{-1}), ΔS° is the entropy change (kJ mol^{-1} K^{-1}), Thus ΔH° and ΔS° can be determined by the slope and intercept. The value of ΔS°, ΔH° and ΔG°, are showed in Table 5. The negative values of free energy change mean spontaneous process with a high affinity of the adsorbate to the surface of adsorbent. The positive value of enthalpy change and standard entropy indicated spontaneous and endothermic nature of adsorption process.

4. CONCLUSIONS

Three activated carbons were prepared from date palm pits using different activating agents: H_3PO_4, $ZnCl_2$, and NaOH. TGA, % ash content, nitrogen adsorption, SEM, pH_{PZC}, and FTIR confirm the thermal stability of activated carbons. S_{BET} ranged between 427.8 and 498.9 m^2/g. The optimum condition for removal of 2,4-D was confirmed at pH7, equilibrium time 24 h and increased with temperature. Maximum adsorption capacities for the three adsorbents were found to be 51.02, 59.77, and 80 mg/g for AP21, AZ21 and AN13, respectively at 25℃. The adsorption of 2,4-D on the prepared activated carbons follow pseudo-second order kinetic model with correlation coefficients reached to 0.9982. Thermodynamic measurements showed spontaneous and endothermic nature of adsorption process.

COMPETING INTERESTS

Authors have declared that no competing interests exist.

REFERENCES

1. Howard PHE. Handbook of environmental fate and exposure data for organic chemicals. Lewis Publishers (Chelsea MI). 1991;145-156.
2. U.S. Environmental protection agency. Technical Fact Sheet on 2, 4- D; 2002. Available:http://www.epa.gov/ogwdw/dwh/t-soc/24-d.html
3. U.S. Environmental protection agency. Air Data: About AQS Hazardous Air Pollutants; 2006. Available:http://www.epa.gov/air/data/help/haqshaps.html

4. U.S. Environmental Protection Agency Reregistration Eligibility Decision for 2,4-D; 2005. Available:http://www.epa.gov/oppsrrd1/REDs/24d-red.pdf
5. U.S. Environmental Protection Agency Technology Transfer Network. Hazard Summary: 2, 4-D (2,4-Dichlorophenoxyacetic Acid) (including salts and esters); 2003.
6. Aungpradit T, Sutthivaiyakit P, Martens D, Sutthivaiyakit S, Kettrup AAF. Photocatalytic degradation of triazophos in aqueous titanium dioxide suspension identification of intermediates and degradation pathways. J Hazard Mater. 2007;146:204–213.
7. Mahvi AH. Application of ultrasonic technology for water and wastewater treatment. Iran J Public Health. 2009; 38(2):1–17.
8. Mahvi AH, Maleki A, Rezaee R, Safari M, Reduction of humic substances in water by application of ultrasound waves and ultraviolet irradiation. Iran J Environ Health Sci Eng. 2009;6(4):233–240.
9. Bazrafshan E, Mahvi AH, Nasseri S, Shaieghi M. Performance evaluation of electrocoagulation process for diazinon removal from aqueous environments by using iron electrodes. Iran J Environ Health Sci Eng. 2007;4(2)127–132.
10. Ballesteros Martin MM, Snchez Pérez JA, Garcia Sanchez JL, Montes DeOca L, Casas Lopez JL, Oller I, Malato Rodriguez S. Degradation of alachlor and pyrimethanil by combined photo-Fenton and biological oxidation. J Hazard Mater. 2008;155:342–349.
11. Dehghani M, Nasseri S, Zamanian Z. Biodegradation of alachlor in liquid and soil cultures under variable carbon and nitrogen sources by bacterial consortium isolated from corn field soil. Iran J Environ Health Sci Eng. 2013;10-21.
12. Dehghani M, Nasseri S, Hashemi H. Study the bioremediation of atrazine under variable carbon and nitrogen sources by mixed bacterial consortium isolated from corn field soil in Fars province of Iran. J Environ Public Health. 2013;10-21.
13. Rajashekara Murthy HM, Manonmani HK. Aerobic degradation of technical hexachlorocyclohexane by a defined microbial consortium. J Hazard Mater. 2007;149:18–25.
14. Ahmad AL, Tan LS, Shukor SRA Dimethoate and atrazine retention from aqueous solution by nanofiltration membranes. J Hazard Mater. 2008;151: 71–77.
15. Hamadi NK, Swaminathan S, Chen XD. Adsorption of paraquat dichloride from aqueous solution by activated carbon derived from used tires. J Hazard Mater. 2004;B112:133–141.
16. Ayar N, Bilgin B, Atun G. Kinetics and equilibrium studies of the herbicide 2,4-dichlorophenoxyacetic acid adsorption on bituminous shale. Chem. Eng. J. 2008;138: 239–248.
17. Date Palm (FAO) [Online] Available:http://www.absoluteastronomy.com/topics/date palm (Accessed 25th August 2009)
18. Dehghani M, Nasseri S, Karamimanesh M. Removal of 2,4-Dichlorophenolyxacetic acid (2,4 D) herbicide in the aqueous phase using modified granular activated carbon. J Enviro Health Sci & Eng. 2014; 12-28.
19. Pirsaheba M, Dargahia A, Hazratib S, Fazlzadehdavilb M. Removal of diazinon and 2,4-dichlorophenoxy-acetic acid (2,4-D)from aqueous solutions by granular-activated carbon. 2014;52:4350–4355.
20. Rodenas MAL, Castello DL, Amoros DC, Solano AL. Preparation of activated carbons from Spanish anthracite II. Activation by KOH. Carbon. 2001;39:751-759.
21. Adekola FA, Adekoge HI. Adsorption of blue dye on activated carbon from rice husk coconut shell and coconut coirpith. Ife Journal of Science. Nigeria. 2005;7(1): 151–157.
22. Hassan AF, Youssef AM, Priecel P. Removal of deltamethrin insecticide over highly porous activated carbon prepared from pistachio Nutshells. Carbon Lett. 2013;14:234-242.
23. Rosas JM, Bedia J, Rodríguez-Mirasol J, Cordero T. HEMP-derived activated carbon fibers by chemical activation with phosphoric acid. Fuel. 2009;88(1):19-26.
24. Yeganeh MM, Kaghazchi T, Soleimani M. Effect of raw materials on properties of activated carbons. Chem Eng Technol. 2006;29:1247-1251.
25. Puziy AM, Poddubnaya OI, Martinez-Alonso A, Suarez-Garcia F, Tascon JMD synthetic carbons activated with phosphoric acid I. Surface chemistry and

ion binding properties. Carbon. 2002;40: 1493–1505.
26. Aguilar C, García R, Soto-Garrido G, Arriagada R. Catalytic wet air oxidation of aqueous ammonia with activated carbon. Appl Catal B. 2003;46:229-237.
27. Ahmad AL, Loh MM, Aziz JA. Preparation and characterization of activated carbon from oil palm wood and its evaluation on methylene blue adsorption. Dyes Pigments. 2007;75:263-272.
28. Budinova T, Ekinci E, Yardim F, Grimm A, Bjornbom E, Minkova V, Goranova M. Characterization and application of activates carbon produced by H_3PO_4 and water vapor activation" Fuel Process Technol. 2006;87:899–905.
29. Foo KY, Hameed BH. Utilization of biodiesel waste as a renewable resource for activated carbon application to environmental problems. Renew. Sustain. Energ. Rev. 2009;13:2495–2504.
30. Molina-Sabio M, Rodriguez-Reinoso F. Role of chemical activation in the development of carbon porosity. Colloids Surf. 2004;241:15–25.
31. Liu QS, Zheng T, Wang P, Guo L. Preparation and characterization of activated carbon from bamboo by microwave-induced phosphoric acid activation. Ind Crops and Prod. 2010;31: (2):233-238.
32. Yang T, Lua AC. Characteristics of activated carbons prepared from pistachio-nut shells by physical activation. J Colloid Interface Sci. 2003;267(2):408-417.
33. Boehm HP. Surface oxides on carbon and their analysis a critical assessment. Carbon. 2002;40(2):145-149.
34. Jankowska H, Świątkowski A, Choma J, Kemp TJ. Active Carbon, E. Horwood, New York; 1991.
35. Rouquerol F, Rouquerol J, Sing KSW Adsorption by powders and porous solid. Academic press, San Diego; 1999.
36. Aroua M, Leong S, Teo L, Daud W. Real time determination of kinetics of adsorption of lead (II) onto shell based activated carbon using ion selection electrode. Bioresour. Technol. 2008;99:5786-5792.
37. Malik R, Ramteke DS, Wate SR. Adsorption malachite green on groundnut shell waste based powdered activated carbon waste management. 2007;27(9): 1129–1138.
38. Njoku VO, Foo KY, Hameed BH. Preparation of activated carbons from Rambutan (*Nephelium lappaceum*) peel by microwave-induced KOH activation for acid yellow 17 dye adsorption. Chem. Eng. J. 2013;383-388.
39. Aksu Z, Kabasakal E. Batch adsorption of 2,4-dichlorophenoxy- acetic acid (2,4-D) from aqueous solution by granular activated carbon Sep. Purif. Technol. 2004;35:223-240.
40. Langumir I. The adsorption of gases on plane surface of glass, mica and platinum. J. Am. Chem. Soc. 1916;1361-1403.
41. Konstantinos F, Garyfallia D. Nikolaos R. Headspace solid- phase microextraction for the gas chromatographic analysis of organ phosphorus insecticides in vegetables. J. AOAC Int. 2007;90:1677-1681.
42. Hsieh CT, Teng H. Influence of mesopore volume and adsorbate size on adsorption capacities of activated carbons in aqueous solutions. Carbon. 2000;38(6):863–869.
43. Susarla S, Bhaskar CV, Bhamidimarri Rao SM. Adsorption-desorption characteristics of some phenoxyaceticacids and chlorophenols in a volcanic soil I. Equilibrium and kinetics. Environmental Technology. 1993;14(2):159–166.
44. Belmouden M, Assabbane A, Ichou YA, Removal of 2.4-dichloro phenoxyacetic acid from aqueous solution by adsorption on activated carbon. A kinetic study. Annales de Chimie Science des Matériaux. 2001;26(2):79–85.

Peer-review history:
The peer review history for this paper can be accessed here:
http://sciencedomain.org/review-history/18810